Petroleum Science 23 (2026) 5914–5927

Contents lists available at ScienceDirect

Petroleum Science

journal homepage: www.keaipublishing.com/en/journals/petroleum-science

Original Paper

Study on the cutting characteristics of different types of abrasive grains on workover bits in the high-temperature environment of the deep wellbore

Jia-Qi Che [a,b], Jia-Qi Qiao [b], Chang-Chang Chen [b], Yi-Han Fan [b], Yun-Fei Chen [b], Yan-Wen Zhang [c,*], Han-Xiang Wang [a,b]

[a] Hubei Key Laboratory of Oil and Gas Drilling and Production Engineering, Yangtze University, Jingzhou, 434000, Hubei, China
[b] College of Mechanical and Electrical Engineering, China University of Petroleum (East China), Qingdao, 266580, Shandong, China
[c] College of Engineering, Ocean University of China, Qingdao, 266100, Shandong, China

A R T I C L E I N F O

Article history:
Received 20 October 2025
Received in revised form
14 November 2025
Accepted 22 March 2026
Available online 25 March 2026

Edited by Min Li

Keywords:
Drilling bit for workover
Abrasive grain
Johnson-Cook constitutive model
Cutting force
Fracture energy

A B S T R A C T

At present, drilling bits for workover under high-temperature conditions are facing technical bottlenecks such as low work efficiency and rapid wear, especially their working characteristics in the high-temperature environment of the deep wellbore need to be improved urgently. To address this issue, first of all, a two-dimensional orthogonal cutting theoretical mechanical model was established based on Oxley's shear theory to analyze the relationship between cutting parameters and working characteristics. Then geometric models of six commonly used abrasive grains in oil fields, namely disc abrasive grain, cylindrical abrasive grain, honeycomb abrasive grain, long strips of abrasive grain, pointed teeth abrasive grain and prismatic abrasive grain, were established. Also, the thermodynamic coupling simulation models in a high-temperature environment of 180 °C were established based on the Johnson-Cook constitutive model. The accuracy of the simulation model was verified through the performance testing equipment of the drilling bit for workover. Single abrasive grain cutting simulation experiments were carried out based on Abaqus, and the cutting characteristics of different structural types of abrasive grains were analyzed from four aspects: cutting mechanism, work safety, work temperature and work efficiency. The analysis results show that: Firstly, the simulation model error of the abrasive grains of the drilling bit for workover is 9.98%, which meets the accuracy requirements for engineering analysis. Secondly, the cutting forces of the honeycomb abrasive grain and the disc abrasive grain are relatively small and have a smooth fluctuation pattern, being 1.27 and 1.45 kN, respectively. Thirdly, during operation, the cutting temperature of the honeycomb abrasive grain is the lowest, at 521 °C, while the cutting temperature of the prismatic abrasive grain is the highest, reaching 612 °C. Fourthly, the crushing ratio work of cylindrical abrasive grain is the lowest, at 14.58 J/mm^3, while that of prismatic abrasive grain is the highest, reaching 15.54 J/mm^3. Based on the analysis of work safety, work temperature and work efficiency, when cutting metal blockages in the high-temperature environment, honeycomb abrasive grain is recommended as the preferred choice. The research content can provide theoretical guidance and technical support for the development of an efficient drilling bit for workover in the high-temperature environment of the deep wellbore.

1. Introduction

60% of the world's new oil and gas reserves come from deep geological layers. Deep and ultra-deep layers have also become the main front for major oil and gas discoveries worldwide. China has 671 billion tons of oil equivalent in deep and ultra-deep oil and gas resources, accounting for 34% of the country's total oil and gas resources (Lu, 2024). Therefore, it is particularly important to

* Corresponding author.
E-mail address: zhangyw0811@163.com (Y.-W. Zhang).
Peer review under the responsibility of China University of Petroleum (Beijing).

https://doi.org/10.1016/j.petsci.2026.03.046
1995-8226/

achieve efficient extraction of deep oil and gas. Efficient development of deep oil and gas resources is a major demand for ensuring national energy security. As the oil and gas production targets become increasingly challenging and the number of oil wells keeps increasing, the number of well repair tasks is also rising. Well repair operations run through the entire life cycle of oil and gas field development and are an important part of ensuring the normal production and stable increase of output of the oil and gas fields. Among them, the drilling bit for workover (also known as the junk mills) is a crucial tool for removing metal obstructions in the wellbore and ensuring the smoothness of the wellbore. As China's oil and gas exploration and development move towards the “low-permeability, deep-sea, offshore, and unconventional” fields (Lei et al., 2019, 2020; Wang et al., 2018; Zhang et al., 2019), the types of oil reservoirs have become more diverse, the wellbore structures are more complex, and the bottom temperatures of deep wells are gradually increasing. Due to the influence of complex environments such as high temperature and high pressure, the drilling bits for workover are confronted with problems such as severe wear, rapid failure and low efficiency. Among them, the cutting teeth (also known as abrasive grain) are the most crucial component of the drilling bit for workover. Their performance directly determines the milling efficiency and service life of the drilling bit for workover. Therefore, conducting research on the grinding and dressing characteristics of cutting teeth of different structural types holds extremely significant importance.

By using the finite element analysis method to simulate the cutting process of the cutting teeth of the drilling bit for workover, and combining with specific experiments to verify the simulation results, this is currently the main method for analyzing and evaluating the working characteristics of the cutting teeth of the drilling bit for workover. Professor Sun Linping and his colleagues established a three-dimensional orthogonal finite element model of the cutting teeth of the junk mills based on cutting mechanics, and analyzed the influence laws of different cutting parameters on the main cutting force (Sun et al., 2018). Yan et al. (2009) established a calculation model for rock crushing work, using the energy perspective to evaluate the drilling efficiency of the drill bit. Abbas (2018) studied the wear mechanism of drill bits. They used finite element and discrete element analysis methods to simulate the wear of drill bits and clarified the wear mechanism of the drill bits. Luo et al. (2023) established a three-dimensional thermal-structural coupling simulation model for the special-shaped teeth of PDC drill bits under high-temperature conditions, and analyzed the rock-breaking characteristics of the special-shaped teeth under such high-temperature conditions. Stowe and Ponder (2014) conducted on-site tests on different types of abrasive grains and analyzed the characteristics and advantages of each type of abrasive grain. Rajabov et al. studied the influence laws of the tooth pitch angle of the cutting teeth on the crushing ratio, work and mechanical response, and clarified the optimal tooth pitch angle for drilling bits and the speed-up mechanism (Dai et al., 2022; Maczura et al., 2015; Rajabov et al., 2012; Rostamsowlat et al., 2018; Zhu and Liu, 2018). Wang et al. (2019) and Zhang et al. (2020) conducted single-tooth rock-breaking experiments using a modified drilling machine, aiming to study the wear mechanism of the single tooth. Furthermore, Baker Hughes, Weatherford and National Oilwell Varco are also dedicated to developing various types of abrasive grains and applying them to well servicing and drilling tools to achieve higher performance in milling operations (Larsen and Garfield, 2013). At present, most scholars and companies are focusing on the research of cutting teeth for rock breaking. However, there is relatively little research on the grinding characteristics of different structural types of abrasive grains when cutting metal blockages in the high-temperature environment of the deep wellbore.

In the early stage, our research team conducted a series of studies on the cutting mechanism and wear mechanism of the drilling bit for workover. Our team first focused on the tooth arrangement of abrasive grains and explored the impact of different tooth arrangement angles on the working characteristics of the drilling bit for workover. Subsequently, based on the thermal coupling effect, we established a simulation model to analyze the heat generation law and temperature control methods of the drilling bit for workover. Through reverse engineering technology, we established a full-scale model of the drilling bit for workover and systematically analyzed the influence of working parameters on the working performance of the drilling bit for workover (Che et al., 2020a, 2020b, 2020c, 2021, 2023). The research shows that it is very important to conduct studies on the milling characteristics of different structural types of abrasive grains.

This paper mainly focuses on the analysis of the cutting characteristics of abrasive grains in the high-temperature environment of the deep wellbore. By combining the finite element simulation analysis and laboratory experiments, it conducts research on the cutting characteristics of abrasive grains of different structural types in deep high-temperature areas. The research results can provide theoretical support and technical guidance for the development of an efficient drilling bit for workover, suitable for the high-temperature environment of the deep wellbore.

2. Cutting theory analysis

Based on Oxley's shear theory, the force conditions of the abrasive grains in the cutting stage of the drilling bit for workover were analyzed, and a two-dimensional orthogonal cutting mechanics model of the shear zone was established (Li et al., 2024). As shown in Fig. 1, under the circumstances of the distribution of multiple physical fields during the cutting process and under the condition of achieving steady-state cutting, the theoretical relationship between the cutting process variables and the output variables was established.

When the cutting process reaches a stable state, the chips are produced at a constant speed. At this point, the chips are in a state of force equilibrium. Analyzing the forces on the chips: the resultant force F_r of the normal force F_{ns} at the shear surface and the shear force F_s at the shear surface, and the resultant force F_{rf1} of the normal force F_{nf1} at the tool-chip interface and the friction force F_{f1} at the tool-chip interface, are a pair of balanced forces. The balance equation is expressed as Eq. (1).

$$\begin{cases} F_{nf1}\sin\alpha - F_{f1}\cos\alpha = F_{ns}\cos\phi - F_s\sin\phi \\ F_{nf1}\cos\alpha + F_{f1}\sin\alpha = F_s\cos\phi + F_{ns}\sin\phi \end{cases} \tag{1}$$

In the formula, α represents the angle of the abrasive grain cloth teeth, and ϕ represents the shear angle (the acute angle formed between the shear surface and the direction of the cutting speed), F_{ns} represents the normal force at the cutting chip surface, F_s represents the shear force at the cutting chip surface, F_r represents the resultant force of the normal force and shear force at the cutting chip surface, F_{nf1} represents the normal force at the tool-chip interface, F_{f1} represents the frictional force at the tool-chip interface, and F_{rf1} represents the resultant force of the normal force and frictional force at the tool-chip interface.

From the fact that the abrasive grains are in a state of uniform cutting, we can conclude: The total cutting force F_r of the abrasive grains, the normal force F_N at the cutting edge of the abrasive grains, the frictional force F_t at the cutting edge of the abrasive grains, as well as the resultant force F_T of these three forces, and

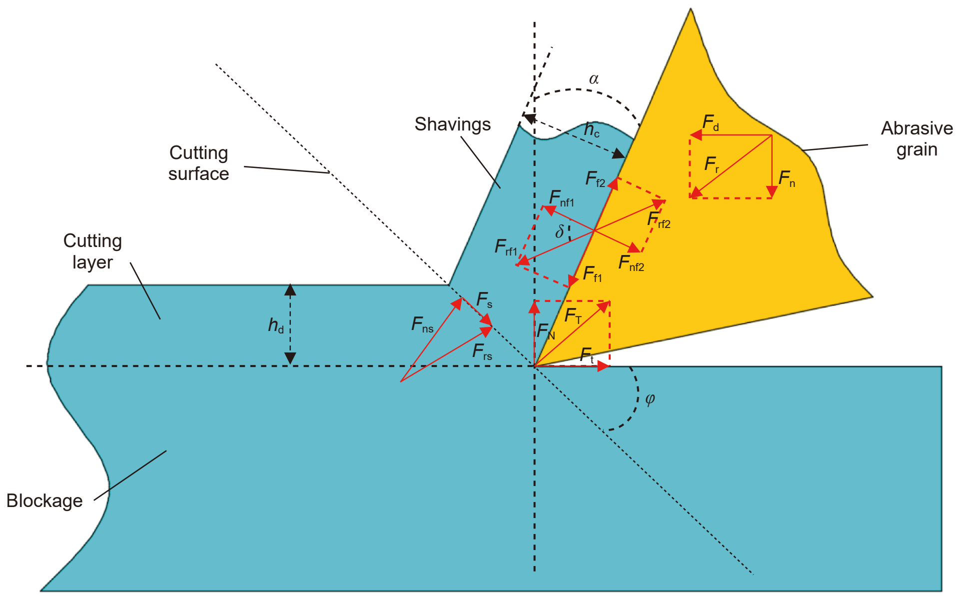

Fig. 1. Mechanical model of cutting process.

the normal force F_{nf2} at the tool-chip interface and the frictional force F_{f2} at the tool-chip interface, as well as their resultant force F_{rf2}, these forces form a balanced force. The total cutting force F_r along the direction of cutting speed and the normal direction of the cutting plane can be decomposed as follows: The cutting force F_d and the normal force F_n establish the equilibrium equation as shown in Eq. (2).

$$\begin{cases} F_d = F_t + F_{nf2}\cos\alpha + F_{f2}\sin\alpha \\ F_n = F_N + F_{f2}\cos\alpha - F_{nf2}\sin\alpha \end{cases} \tag{2}$$

In the formula, F_r represents the total cutting force of the abrasive grains, F_N represents the normal force at the cutting edge of the abrasive grains, F_t represents the frictional force at the cutting edge of the abrasive grains, F_T represents the resultant force of the normal force and frictional force at the cutting edge of the abrasive grains, F_{nf2} represents the resultant force of the normal force and frictional force at the tool-chip interface, F_d represents the main cutting force, and F_n represents the normal cutting force.

From the shear force formula of the material, we obtain Eq. (3).

$$F_s = \tau_s S_a = \frac{\tau_s h_d l}{\sin\phi} \tag{3}$$

In the formula, τ_s represents the shear strength of the metal block material, S_a represents the shear area, h_d represents the cutting depth, l represents the cutting width, and δ represents the friction angle, F_s represents the shear force at the shear surface.

From the above equation, we can obtain the normal force F_{ns} of the abrasive grains and the main cutting force F_{ds} of the abrasive grains as Eq. (4):

$$\begin{cases} F_{ds} = F_t + \dfrac{\tau_s h_d l\cos(\delta-\alpha)}{\sin\phi\cos(\delta+\phi-\alpha)} \\ F_{ns} = F_N + \dfrac{\tau_s h_d l\sin(\delta-\alpha)}{\sin\phi\cos(\delta+\phi-\alpha)} \end{cases} \tag{4}$$

In the formula, F_{ds} represents the main cutting force of the abrasive grains, and F_{ns} represents the normal cutting force of the abrasive grains.

The abrasive grains of the drilling bit for workover perform a circular cutting motion in the well. Let the diameter of this circular cutting motion be d. Then the torque generated by the abrasive grains is Eq. (5):

$$M = F_{ds}\frac{d}{2} = \frac{d}{2}\left(F_t + \frac{\tau_s h_d l\cos(\delta-\alpha)}{\sin\phi\cos(\delta+\phi-\alpha)}\right) \tag{5}$$

Based on the above mechanical analysis of the cutting process, it can be concluded that: The cutting force generated by the abrasive grains of the drilling bit for workover during the cutting process increases linearly with the increase in cutting width and depth, and undergoes stepwise periodic fluctuations with the change in the tooth angle of the abrasive grains. The cutting force of the abrasive grains is also influenced by factors such as the friction angle of the material, the shear angle, the friction coefficient between the tool and the material, and the shear strength of the material.

3. Cutting simulation of abrasive grain

3.1. Different structural types of abrasive grains

At present, the oilfield mainly uses the six types of abrasive grains shown in Fig. 2 for the milling operation of the underground metal blockages. These include disc abrasive grain, cylindrical abrasive grain, honeycomb abrasive grain, long strip abrasive grain, pointed teeth abrasive grain and prismatic abrasive grain. Based on the geometric dimensions of the abrasive grains, geometric models of the six different structural types of abrasive grains are established, providing a model basis for the subsequent analysis of the milling characteristics of different structural types of abrasive grains.

3.2. Constitutive model of metal cutting layer material

The titanium alloy material can still maintain the required strength under high-temperature conditions. Therefore, in the simulation process, titanium alloy material is used as the cutting layer material. The parameters of the titanium alloy material, as

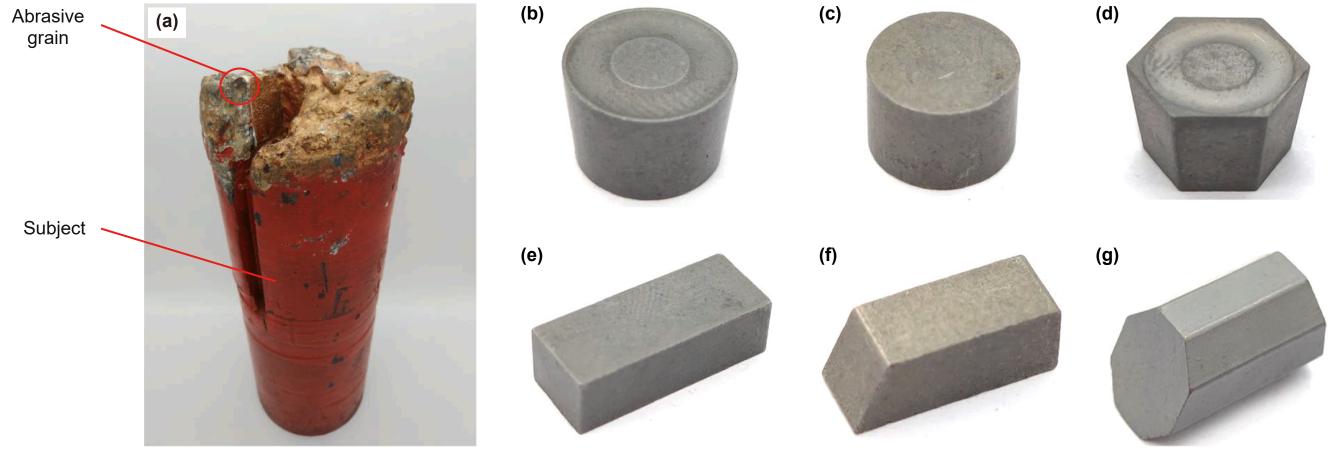

Fig. 2. Different structural types of abrasive grains. **(a)** Drilling bit for workover; **(b)** Disc abrasive grain; **(c)** Cylindrical abrasive grain; **(d)** Honeycomb abrasive grain; **(e)** Long strips of abrasive grain; **(f)** Pointed teeth abrasive grain; **(g)** Prismatic abrasive grain.

determined by referring to reference (Yang, 2022), are shown in Table 1.

During the process of grinding and milling metal obstructions in the well, the drilling bit for workover undergoes significant material deformation and damage. The Johnson-Cook model comprehensively considers the strain hardening effect (Xiao et al., 2024), strain rate strengthening effect, and thermal softening effect of the material, successfully coupling the three core physical mechanisms in the cutting process: work hardening caused by extreme strain, strain rate strengthening caused by extremely high strain rates, and thermal softening caused by adiabatic temperature rise. In particular, its ability to describe thermal softening and failure makes it the preferred model for predicting cutting force, chip morphology, and cutting temperature, suitable for simulating the large deformation and damage process of metal materials. Therefore, the Johnson-Cook model is adopted as the constitutive model for the metal blockage material, and the Johnson-Cook damage criterion is introduced (Ljustina et al., 2014). The Johnson-Cook model is as follows:

$$\sigma = (A + B\varepsilon^n)\left(1 + C\ln\frac{\dot{\varepsilon}}{\dot{\varepsilon}_0}\right)\left[1 - \left(\frac{T - T_r}{T_{\text{melt}} - T_r}\right)^m\right] \tag{6}$$

$$D = \int \frac{\mathrm{d}\bar{\varepsilon}_{\text{p}}}{\bar{\varepsilon}_{\text{p}}^f} \tag{7}$$

$$\begin{aligned}\bar{\varepsilon}_{\text{p}}^f = &\left[d_1 + d_2 \exp\left(d_3 \frac{\varepsilon_{\text{p}}}{\varepsilon_{\text{Mises}}}\right)\right] \\ &\times \left[1 + d_4 \ln\left(\frac{\dot{\varepsilon}_{\text{p}}}{\dot{\varepsilon}_0}\right)\right] \times \left(1 + d_5 \frac{T - T_{\text{r}}}{T_{\text{melt}} - T_{\text{r}}}\right)\end{aligned} \tag{8}$$

In the formula, σ represents the flow stress, ε represents the equivalent plastic strain, $\dot{\varepsilon}$ represents the loading strain rate, $\dot{\varepsilon}_0$ represents the reference strain rate, T represents the experimental temperature, T_{melt} represents the material melting temperature, T_{r} represents the ambient temperature, A represents the reference loss strain coefficient, B is the stress triaxiality coefficient, n is the stress triaxiality index, C is the strain rate sensitivity coefficient, m is the temperature sensitivity coefficient, D is the damage parameter, $\mathrm{d}\bar{\varepsilon}_{\text{p}}$ is the equivalent plastic strain increment of the integration element, $\bar{\varepsilon}_{\text{p}}^f$ is the critical equivalent plastic strain, and d_1–d_5 are the failure parameters.

Based on the material properties (Zhou et al., 2019), the Johnson-Cook constitutive model parameters of the titanium alloy material are determined through calculation (Table 2).

3.3. Cutting simulation model for single abrasive grain

Based on the above abrasive grain geometric model and the mechanical performance parameters of the metal blockage, taking the abrasive grain cutting unit of the drilling bit for workover as the research object, a three-dimensional thermal-coupled simulation model for abrasive cutting was established (Qian et al., 2020; Ye et al., 2019; Zheng et al., 2020). The abrasive grain cutting unit is approximately linear cutting. According to the actual working conditions of abrasive grain tooth distribution, the size of the metal blockage is established as 25 mm × 15 mm × 10 mm, and fixed constraints are applied to the lower surface and the surrounding area of the metal blockage. A reference point is set at the center of the bottom of the abrasive grain, and the entire abrasive grain is set as a solid body. The three-dimensional orthogonal cutting thermal-thermal coupling simulation model constructed simultaneously satisfies the following assumptions.

(1) The cutting tool is set as a steel body, and only the heat conduction effect of the cutting tool is considered.
(2) Ignore the changes in the metallographic structure and other chemical changes of the material that occur during the cutting process due to temperature variations.
(3) The material of the object being machined is isotropic.
(4) Ignoring the vibrations of the cutting tool and the workpiece during the cutting process.

Table 1
Parameters of the constitutive model for titanium alloy materials.

Density, kg/m^3	Elastic modulus, GPa	Poisson's ratio	Thermal conductivity, W/(m·K)	Specific heat capacity, J/(kg·K)	Melting point temperature, °C
4430	110	0.3	6.8	565	1660

Table 2
Parameters of the constitutive model for titanium alloy materials.

A, MPa	*B*, MPa	*C*	*m*	*n*	T_{melt}, °C	d_1	d_2	d_3	d_4	d_5
875	793	0.01	0.71	0.386	1560	−0.09	0.27	−0.48	0.014	0.55

For the meshing of the bottom layer of the metal blockage, hexahedral meshes are used. The size of the bottom layer mesh of the blockage is determined to be 1 mm. The meshes on the top layer of the metal blockage are densified. To ensure the simulation accuracy, a mesh independence test is conducted on the single abrasive particle cutting simulation model, as shown in Fig. 3. The mesh size of the encrypted area in the cutting layer is set to 0.1–0.9 mm, respectively, and the calculation time of the simulation model under different mesh sizes is determined. The torque generated by the abrasive particle is used as the evaluation index, and the simulation results of abrasive particle cutting and the experimental results are compared to determine the calculation accuracy of the simulation model under different mesh sizes. Through the verification of the accuracy of different mesh sizes, when the mesh size of the simulation model increases from 0.1 to 0.3 mm, the calculation time decreases sharply from 13680.5 to 9337.9 s. Then, as the mesh size increases from 0.3 to 0.9 mm, the calculation time decreases slowly from 9337.9 to 4780.3 s. On the other hand, when the mesh size of the simulation model increases from 0.1 to 0.2 mm, the relative error increases slowly from 7.8% to 8.3%, and then as the mesh size increases from 0.2 to 0.9 mm, the relative error increases rapidly from 8.3% to 23.6%. Considering the calculation efficiency and accuracy of the simulation model, the size of the encrypted grid of the cutting layer is determined to be 0.2 mm, with a grid number of 129,300. The top grid is densified for better simulation accuracy. The abrasive particle uses tetrahedral meshes, with a grid number of 5780. The grid diagram of the abrasive particle cutting simulation model is established.

By adjusting the working conditions of the drilling bit for workover for cutting metal blockages under high-temperature environments, a three-dimensional orthogonal thermal coupling simulation model of abrasive grains, as shown in Fig. 4, was established. The abrasive grains were placed with a negative toothing angle of 8°. This angle resulted in a large amount of debris removal by the abrasive grains, and the working process of the abrasive grains was smooth. The bottom and surrounding areas of the metal blockage are subject to completely fixed constraint boundary conditions. The temperature-displacement coupled penetration contact algorithm is used to simulate the thermal coupling working process of the abrasive grains. At the same time, a 180 °C temperature field is applied to the entire model to simulate the high-temperature environment in deep oil and gas wells. The actual working conditions during the cutting of the drilling bit for workover were established. A reference point is set at the tip of the abrasive grain, and the drilling pressure in the *y* direction is applied to the reference point to simulate the drilling pressure of the drill bit, and the cutting speed *v* in the *x* direction is applied to the reference point to simulate the cutting speed of the drill bit. The cutting speed of the abrasive grain is calculated based on the rotational speed of the well servicing drill bit. The cutting

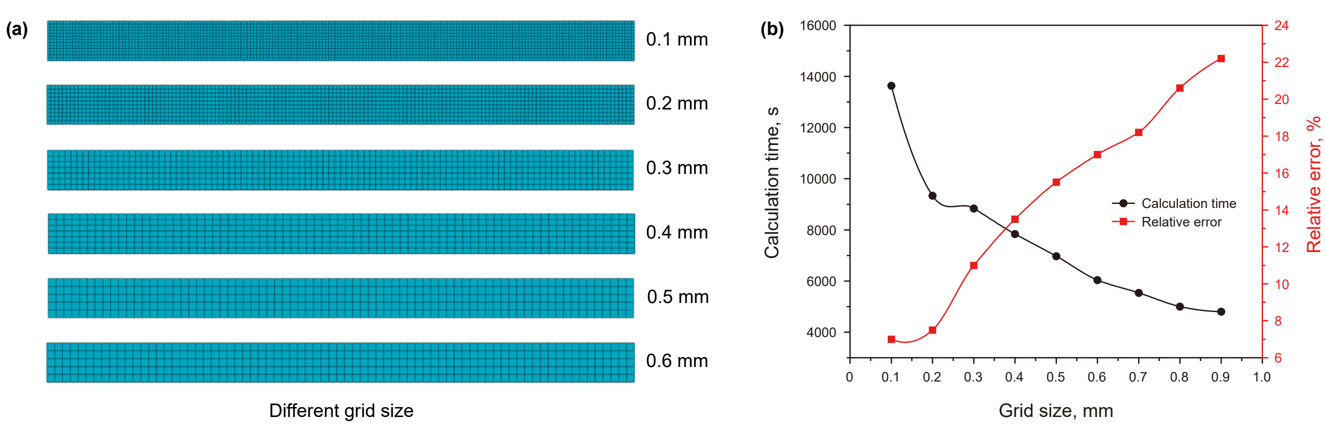

Fig. 3. Verification of grid accuracy under different sizes. **(a)** Different-sized cutting layer grid diagrams; **(b)** Grid accuracy verification.

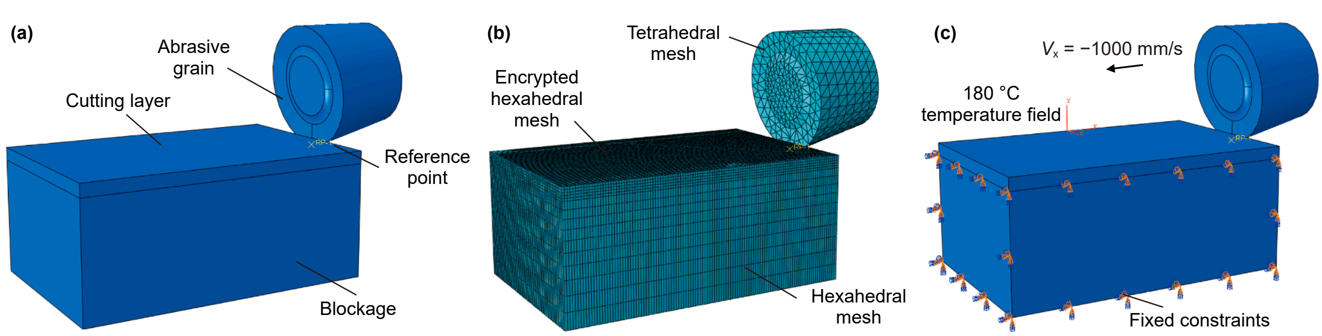

Fig. 4. Three-dimensional orthogonal thermal-coupling simulation model of abrasive grains. **(a)** Simulation model; **(b)** Simulation mesh; **(c)** Simulation environment.

speed of the abrasive grain is 1000 mm/s. The meshing of the metal blockage bottom is divided using hexahedral meshes, and the size of the bottom mesh of the blockage is determined to be 1 mm. The meshing of the top of the metal blockage is divided by encryption, and the size of the encrypted mesh is determined to be 0.2 mm based on the mesh independence test. The number of meshes is 129,300, and the encryption division of the top mesh is carried out to obtain better simulation accuracy. The abrasive grain uses tetrahedral meshes, with a mesh number of 5,780. The grid map of the abrasive grain cutting simulation model is established. By changing the type of abrasive grains, a simulation experiment on single abrasive particle cutting for drilling bit for workover was conducted.

4. Cutting experiment analysis

In order to verify the accuracy of the three-dimensional orthogonal thermal coupling simulation model, based on the experimental system for milling tools independently developed by China University of Petroleum (East China), a cutting experiment of a single abrasive grain drilling bit for workover was carried out. The experimental system for milling tools consists of a drilling bit for workover performance testing platform, a frequency conversion speed regulation module, a high-speed camera module, a drilling pressure control module, a signal acquisition and display module, and a drilling bit for workover module. The frequency conversion speed regulation module is used to adjust the rotational speed of the drilling, milling and drilling tools, while the thrust control module is used to regulate the thrust of the drilling, milling and drilling tools to simulate the effects of different drilling pressures. The adjustable range of drilling pressure is 0–20 kN, and the adjustable range of rotational speed is 20–200 r/min. The signal acquisition and display module display the rotational speed and torque data of the drilling, milling and drilling tools in real time. The well drilling bit module is specially equipped with a detachable single cutting tooth joint to meet the requirements of single tooth cutting experiments. The single abrasive cutting experiment process is shown in Fig. 5.

In order to verify the accuracy of the simulation results, the torque generated by a single abrasive grain drilling bit during the experiment was recorded through the signal acquisition display module, and the torque produced by a single abrasive grain cutting was obtained through the single abrasive grain cutting simulation model. The torque curves obtained from the experiment and the simulation are shown in Fig. 6.

The average value of the single abrasive grain cutting torque during the stable cutting stage obtained through simulation is 37.34 N·m, while the average value obtained through experiment is 41.48 N·m. The error between the simulation results and the experimental results is 9.98%, indicating that the single abrasive grain cutting simulation model is relatively accurate and can meet the basic engineering analysis accuracy requirements. During the experiment, the torque of the single abrasive grain drilling bit increased rapidly at first, reaching 31.20 N·m at the 33rd millisecond. Then the experimental torque remained stable and fluctuated within the stable cutting range of 31.20 to 50.36 N·m. For the simulation torque curve, the trend was basically the same as that of the experimental torque curve. The simulation torque first increased sharply and reached 32.05 N·m at the 25th millisecond. Then the experimental torque remained stable and fluctuated within the stable cutting range of 32.05 to 47.23 N·m. The experimental observation results show that the torque data obtained have a significant lag on the time axis compared to the simulated torque. This is mainly due to the inherent response delay of the signal acquisition and transmission system. However, the experimental torque curve and the simulated torque curve have a

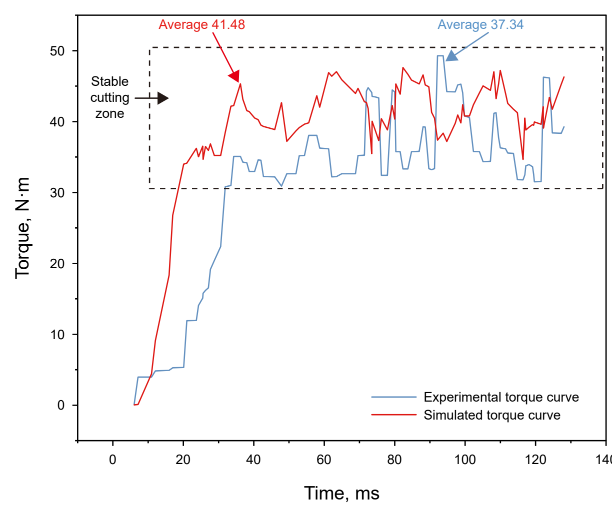

Fig. 6. Cutting torque curve of single abrasive grain.

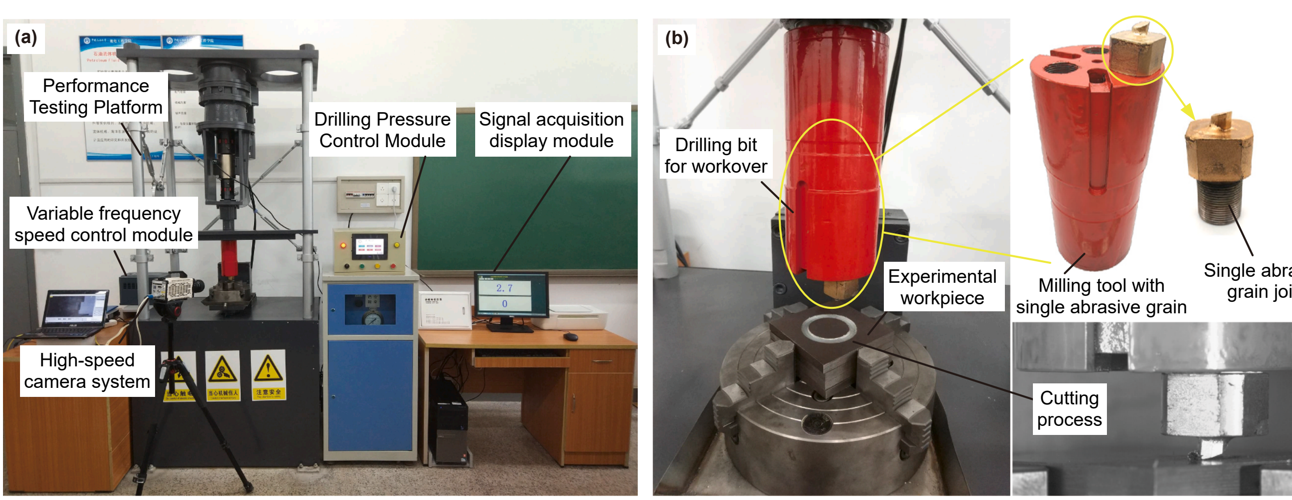

Fig. 5. Cutting experiment process of single abrasive grain. (**a**) Experimental system for milling tools; (**b**) Milling tool with single abrasive grain.

basically consistent trend of change, which further demonstrates the accuracy of the simulation model.

In addition, the variation trends of the experimental and simulation torque curves are in agreement with the mechanical analysis model of the abrasive grains. This further verifies the accuracy of the mechanical analysis model of the drilling bit for workover in Section 2. Specifically, under the action of the drilling pressure, the abrasive grains at the drilling bit for workover gradually get pressed into the surface of the experimental workpiece. The cutting depth h and cutting width b of the abrasive grains gradually increase, thus resulting in the phenomenon that the torque of the workover bit with a single cutting tooth increases sharply first. As the abrasive grains gradually penetrate the experimental workpiece, due to the resistance of the elastic-plastic deformation of the experimental workpiece and the friction force between the front cutting face of the abrasive particle and the cutting layer, the increasing resistance hinders the further pressing of the abrasive grains into the experimental workpiece. Therefore, the cutting depth h and cutting width b of the abrasive grains no longer increase, and the torque of the workover bit with a single cutting tooth gradually stabilizes, and the cutting process enters the stable cutting stage.

5. Result analysis and discussion

5.1. Analysis of cutting mechanism

The cutting process of the abrasive grains welded at the bottom of the drilling bit for workover is shown in Fig. 7. Firstly, as shown in Fig. 7(a), during the fracturing stage, under the combined action of the drilling pressure and torque, the cutting edge at the bottom of the abrasive grain collides and squeezes the metal blockage. Since the initial contact is not firm, the depth of the abrasive grain penetrating into the blockage is not large. The cutting edge of the abrasive grain slides on the surface of the metal blockage, causing the metal blockage to undergo certain elastic deformation, and cracks appear on the surface of the blockage due to the impact. As the drilling pressure between the abrasive grain and the blockage surface continues to increase, as shown in Fig. 7(b) in the penetration stage, the depth of the abrasive grain penetrating into the blockage also increases. The surface material of the blockage gradually transitions from elastic deformation to plastic deformation. Under the combined action of torque and drilling pressure, the stress generated by the abrasive grain gradually exceeds the strength limit of the material. At this time, due to the compression, the surface material of the blockage undergoes fragmentation, generating small particle-like chips. As the drilling pressure further increases, as shown in Fig. 7(c) in the chip formation stage, the cutting edge of the abrasive grain penetrates into the surface layer of the blockage, and the cutting thickness reaches a certain value. At this time, under the action of torque, the abrasive grain continues to move forward, and the surface layer of the blockage undergoes a slip phenomenon. The slip causes the surface layer material to flow towards the front cutting face and both sides of the abrasive grain, and a groove appears on the surface of the cut-off blockage. The shear stress generated by the abrasive grain under the action of torque is greater than the critical shear stress of the material, causing plastic flow and bulging on the material surface, resulting in the separation of the surface layer of the blockage from the base material. As the drilling pressure and torque continue to increase, as shown in Fig. 7(d) in the stable cutting stage, the depth of the abrasive grain penetrating into the blockage increases, and the friction resistance between the abrasive grain and the chip on the front cutting face, as well as the plastic deformation of the blockage, also increase. Eventually, in the vertical direction, they reach equilibrium with the drilling pressure, and the drilling pressure reaches a stable state. Under the action of torque, the abrasive grain moves forward, and the cut-off layer is subjected to slip under the compression of the abrasive grain along the shear plane, forming chips that flow out along the front cutting face of the abrasive grain, and the cutting motion process gradually becomes stable.

Based on the verification of the model of abrasive cutting of metal blockages, six types of abrasive cutting simulation models were successively established: disc abrasive grain, cylindrical abrasive grain, honeycomb abrasive grain, long strip abrasive

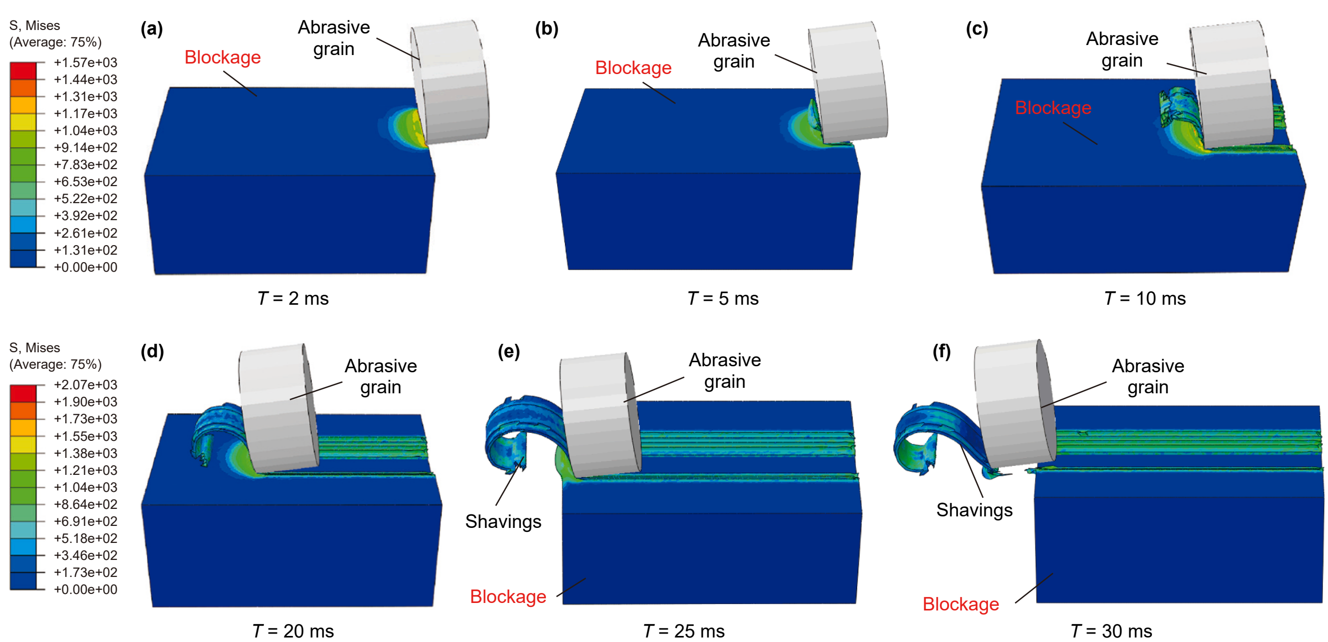

Fig. 7. Cutting process of the abrasive grains welded at the bottom of the drilling bit for workover. **(a)** Collision stage; **(b)** Entry stage; **(c)** Crumb stage; **(d)** Stable cutting stage; **(e)** and **(f)** separation stages.

grain, pointed teeth abrasive grain and prismatic abrasive grain. The cutting characteristics of different types of abrasive grains in the high-temperature environment of the deep wellbore were explored, and the cutting characteristics of different types of abrasive grains are shown in Fig. 8.

As shown in Fig. 8 of the abrasive cutting characteristics, the maximum contact stress areas during the abrasive cutting process all occur at the cutting edges on both sides of the abrasive grains. Among them, the honeycomb abrasive grains with a circular groove have the minimum contact stress of 160 MPa during the cutting process. The contact stress generated by the honeycomb abrasive grains during the cutting process is much lower than the strength limit of the material, which can effectively prevent macroscopic fracture and cracking, and at the same time maintain the structural integrity throughout the wear life. For the pointed tooth abrasive grains during the cutting process, due to the large contact area between the front cutting face of the abrasive particle and the chip, the maximum contact stress generated by the disc-shaped abrasive grains during the cutting process is 318 MPa. High contact stress means a huge amount of frictional work, which will instantly generate a large amount of heat, resulting in a decrease in the hardness and wear resistance of the abrasive particle. The stress generated by the other four types of abrasive grains during the cutting process is approximately the same.

The shape of the chips affects the chip return process. For the simulation model of single abrasive cutting under high-temperature conditions and thermal-physical coupling effects, the chip formation process and the chip formation mechanism are analyzed. Based on the simulation model established in the previous text, the chips produced by each structural type of abrasive grains were extracted, and a comparative analysis of the chip shapes generated by different structural types of abrasive grains was conducted, as shown in Fig. 9.

As shown in Fig. 9, during the chip formation process under the action of thermal coupling, as the abrasive grains move, the edge of the rolled-up chip shows obvious serrations, and an adiabatic shear band with a certain inclination angle is generated between adjacent serrations. As the abrasive grains continue to move, the shear band and the grid undergo significant deformation, thereby continuously and periodically generating serrations. The adiabatic shear band produced in the high-temperature area is an important reason for the formation of serrations. Disc and cylinder-shaped abrasive grains tend to produce large-sized and highly curled spiral chips; honeycomb-shaped abrasive grains generate small-sized fragmented chips; long strips, pointed teeth, and prismatic abrasive grains mostly produce large-sized and low-curvedness long ribbon-shaped chips. Due to the influence of the contact area with the chip, the width of the chips produced during the cutting process of long strips, prisms, and pointed teeth is large, and they are not prone to breaking, thus easily forming long and large-volume chips. Large-volume chips are more difficult to return with the cutting fluid, and it is necessary to optimize the hydraulic parameters to improve the return ability of the chips. When cutting, the contact surface of honeycomb abrasive grains is in the shape of a V, with a small contact area, and the chips formed during cutting are in a granular state, with a small volume, and they are easy to return to the ground with the cutting fluid.

5.2. Analysis of work safety

The fluctuation of cutting force is an important evaluation index reflecting the work safety of the drilling bit for workover during the grinding particle cutting process. Through the established abrasive grain cutting simulation model, the cutting force of different structural types of grinding particles was extracted, and the fluctuation of cutting force for different structural types of abrasive grain is shown in Fig. 10. As can be seen from Fig. 10, during the simulation of abrasive grain cutting, due to the initial collision between the front cutting edge of the abrasive grain and the cutting layer, the main cutting force did not exceed the yield strength of the metal cutting layer. Therefore, the main cutting force showed a phenomenon of rapidly increasing first, and after

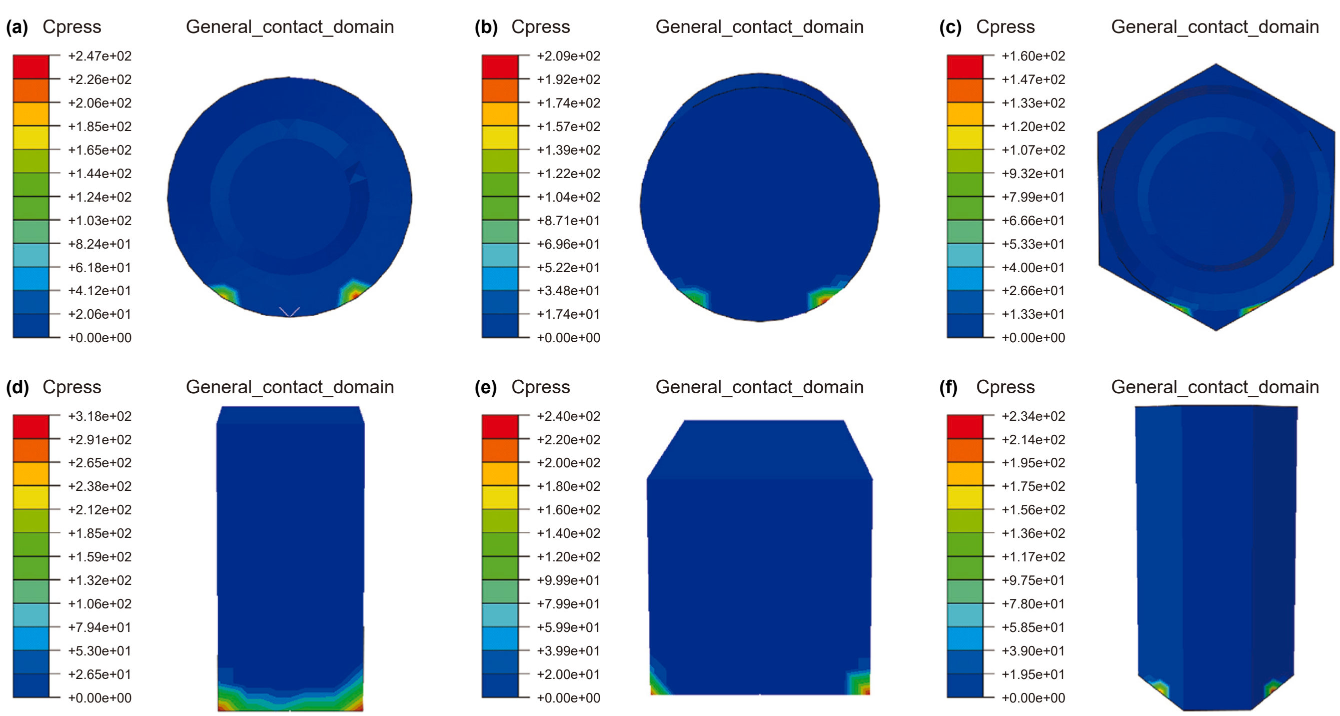

Fig. 8. Cutting characteristics of various abrasive grains. **(a)** Disc abrasive grain; **(b)** Cylindrical abrasive grain; **(c)** Honeycomb abrasive grain; **(d)** Pointed teeth abrasive grain; **(e)** Long strips of abrasive grain; **(f)** Prismatic abrasive grain.

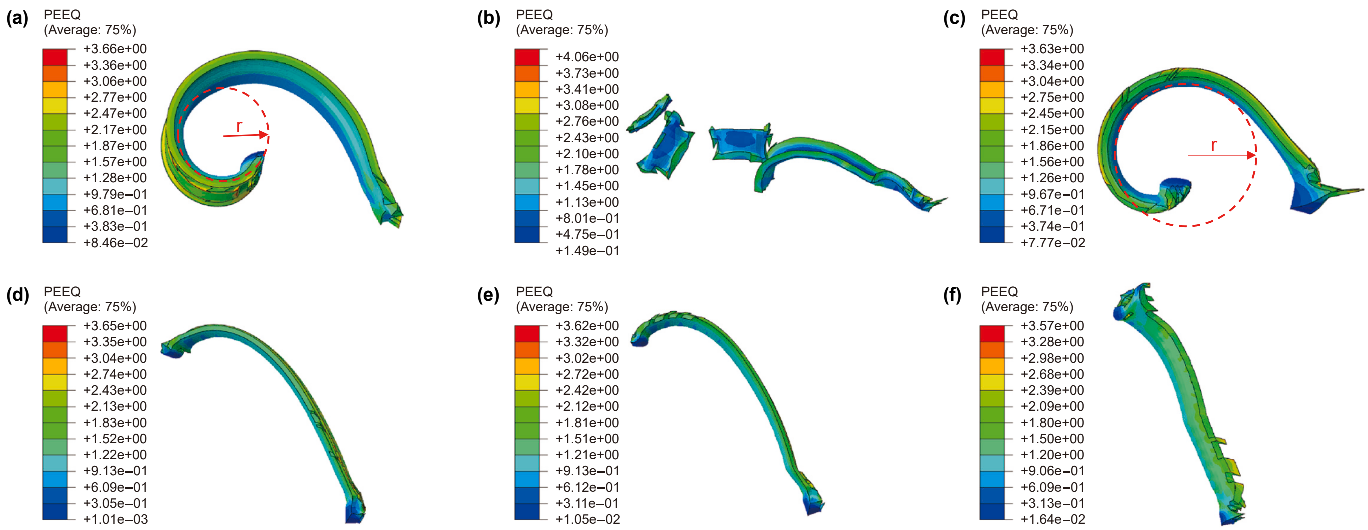

Fig. 9. Chip shapes generated by various abrasive grains. **(a)** Disc abrasive grain; **(b)** Honeycomb abrasive grain; **(c)** Cylindrical abrasive grain; **(d)** Long strips of abrasive grain; **(e)** Pointed teeth abrasive grain; **(f)** Prismatic abrasive grain.

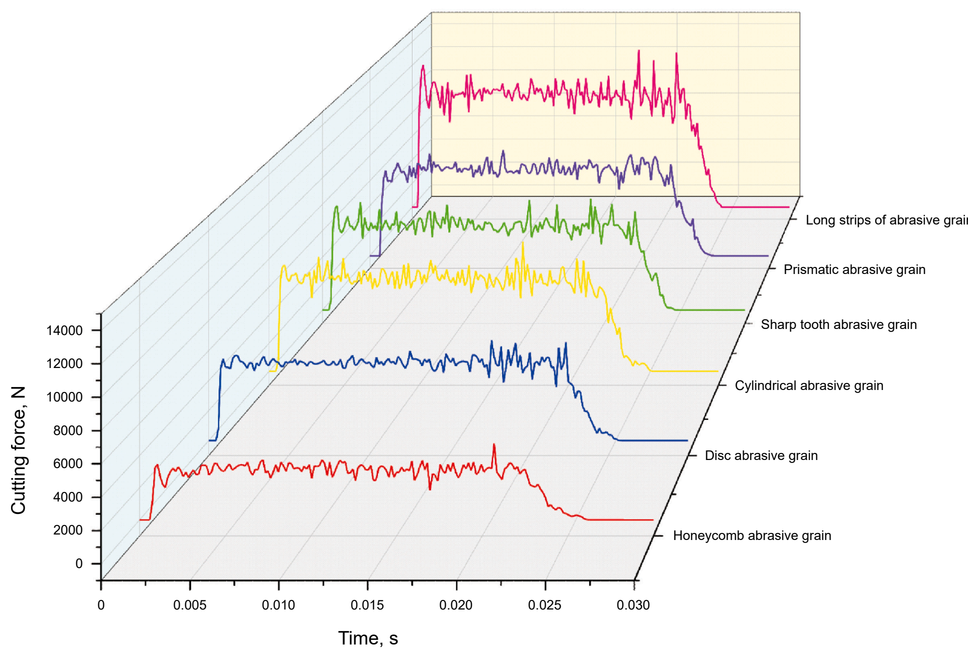

Fig. 10. Main cutting forces of various abrasive grains.

reaching a certain peak, the metal cutting layer underwent shear slip deformation, and the main cutting force would decrease to a certain extent. As the cutting gradually entered the stable cutting stage, the magnitude of the main cutting force fluctuated within a certain range.

By extracting the main cutting force diagrams of the abrasive grains, a comparison Table 3 was established to compare the average cutting force, maximum cutting force, minimum cutting force, and the fluctuation amplitude of the cutting force during the stable cutting stage of the cutting forces generated by abrasive grains of different structural types. A comparative analysis of the cutting force characteristics of abrasive grains of different structural types was conducted.

By extracting the main cutting force values of each structural type of abrasive grains during the cutting process, and based on the cutting forces of the abrasive grain between 0.005 and 0.015 s, the average values and amplitude diagrams of the main cutting forces of the abrasive grain during the stable cutting stage were established, as shown in Fig. 11.

From Fig. 11 and Table 3, it can be seen that under high-temperature conditions, for the disc abrasive and honeycomb abrasive, after entering the stable cutting stage, the fluctuation range of cutting force is relatively small, being 1.45 and 1.27 kN, respectively. The cutting process is more stable, which is conducive to ensuring the stability of the cutting. However, for the prism abrasive and the long strip, the fluctuation range of cutting force during the stable cutting stage is larger, being 2.19 and 3.07 kN, respectively. The cutting process is more violent in vibration, which affects the stability of the cutting. At the same time, the larger cutting force and fluctuation amplitude will increase the

Table 3
Cutting forces of different types of abrasive grains.

Abrasive grain	Average cutting force, N	Maximum cutting force, N	Minimum cutting force, N	Amplitude of fluctuation, N
Disc abrasive grain	5058	5708	3872	1836
Cylindrical abrasive grain	6479	8151	5181	2970
Honeycomb abrasive grain	3094	3729	2423	1306
Pointed teeth abrasive grain	6325	7962	4973	2989
Long strips of abrasive grain	9323	11,269	8041	3228
Prismatic abrasive grain	6842	7936	5712	2224

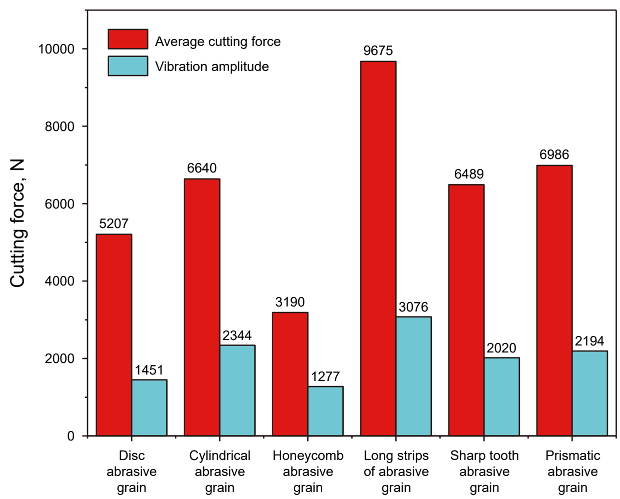

Fig. 11. Amplitude diagrams of the main cutting forces for various abrasive grains.

load during the cutting process, affecting the stability of the cutting and intensifying the wear of the drilling bit for workover. Due to the different contact areas between the abrasive grains and the cutting edge, as well as the chips for different structural types, the cutting forces during the abrasive cutting process vary significantly in value. The fluctuation of the cutting force reflects the stability of the abrasive grains in the cutting process of the drilling bit for workover. Based on the simulation results, it can be concluded that the cutting forces of the disc abrasive grain and the honeycomb abrasive grain are smaller and have less fluctuation during the cutting process, which can ensure the stable operation of the cutting process and prevent the failure of the drilling bit for workover due to vibration. When selecting abrasive grain from the perspective of cutting stability, disc abrasive grain and honeycomb abrasive grain should be given priority.

5.3. Analysis of work temperature

Temperature has a direct impact on the performance of metal materials. Due to the working environment of deep high temperature, the crystal boundaries and crystal structures within the metal materials change, and the interatomic bonding force weakens, resulting in a decrease in the strength of the metal materials, which will directly affect the service life of the abrasive grain of the drilling bit for workover. Therefore, it is very important to conduct temperature analysis during the grinding process of the drilling bit for workover abrasive grain. Based on the grinding simulation model of abrasive grain in the high-temperature of the deep wellbore environment established in the previous text, the temperature fields of different structural types of abrasive grains are extracted, and the temperature distribution characteristics of different structural types of abrasive grains are obtained, as shown in Fig. 12. As can be seen from Fig. 12, since the heat generated during the grinding process of the abrasive grains mainly comes from the friction between the metal chips in the second deformation zone and the rake face of the abrasive grain, the high-temperature area of the drilling bit for workover abrasive grain is mainly distributed in the contact area between the rake face of the abrasive grain and the metal blockage chips, and the high-temperature area is mainly concentrated at the rake face of the abrasive grain.

Among them, the annular grooves of the honeycomb abrasive grain and the disc abrasive grain play a very effective role in heat dissipation. The larger heat dissipation area ensures that the temperature of the honeycomb abrasive grain is the lowest during the cutting process. While the long strips of abrasive grain and the prismatic abrasive grain have a large contact area with the chip, and a small heat dissipation area, resulting in the accumulation of heat on the front cutting surface of the abrasive grain during cutting, thus forming high temperatures.

In order to better analyze the heat generation situation of different structural types of abrasive grains, from the established model mentioned above, the highest temperatures of different structural types of abrasive grains were extracted for analysis, and the highest temperature diagrams of different structural types of abrasive grains were obtained, as shown in Fig. 13. From Fig. 13, it can be seen that under the same working conditions, the prismatic abrasive grain have the highest temperature during cutting, with a maximum temperature of 612 °C. The honeycomb abrasive grain and the disc abrasive grain have the lowest maximum temperatures during cutting, which are 521 and 529 °C, respectively. This is because the honeycomb abrasive grain and the disc abrasive grain have a recessed texture structure in their structure, which increases the heat dissipation area of the cutting tool and promotes the dissipation of the accumulated heat on the front cutting surface of the abrasive grains during cutting, thereby preventing the accumulation of heat on the front cutting surface of the abrasive grains and forming local high temperatures. The simulation results show that the maximum temperature difference between the honeycomb abrasive and the prism abrasive is 90 °C. Due to the influence of the high-temperature environment, the chemical composition of the material changes, and the abrasive front cutting surface and the chip are prone to undergo oxidation reactions. Under the action of the drilling pressure, the chip is compressed and sintered, and an oxide layer forms on the abrasive front cutting surface. The formation of the oxide layer reduces the friction between the abrasive and the chip, causing the drilling bit for workover to easily slip when cutting through obstructions, thereby increasing the difficulty of removing the obstructions. Therefore, controlling the working temperature of the drilling bit for workover is the key to reducing abrasive failure and extending the service life of the drilling bit for workover.

By analyzing the cutting temperatures of different structural types of abrasive grains, it can be concluded that the cutting temperature of prismatic abrasive grains is the highest during cutting. This indicates that prismatic abrasive grain has the poorest heat dissipation performance when milling down metal

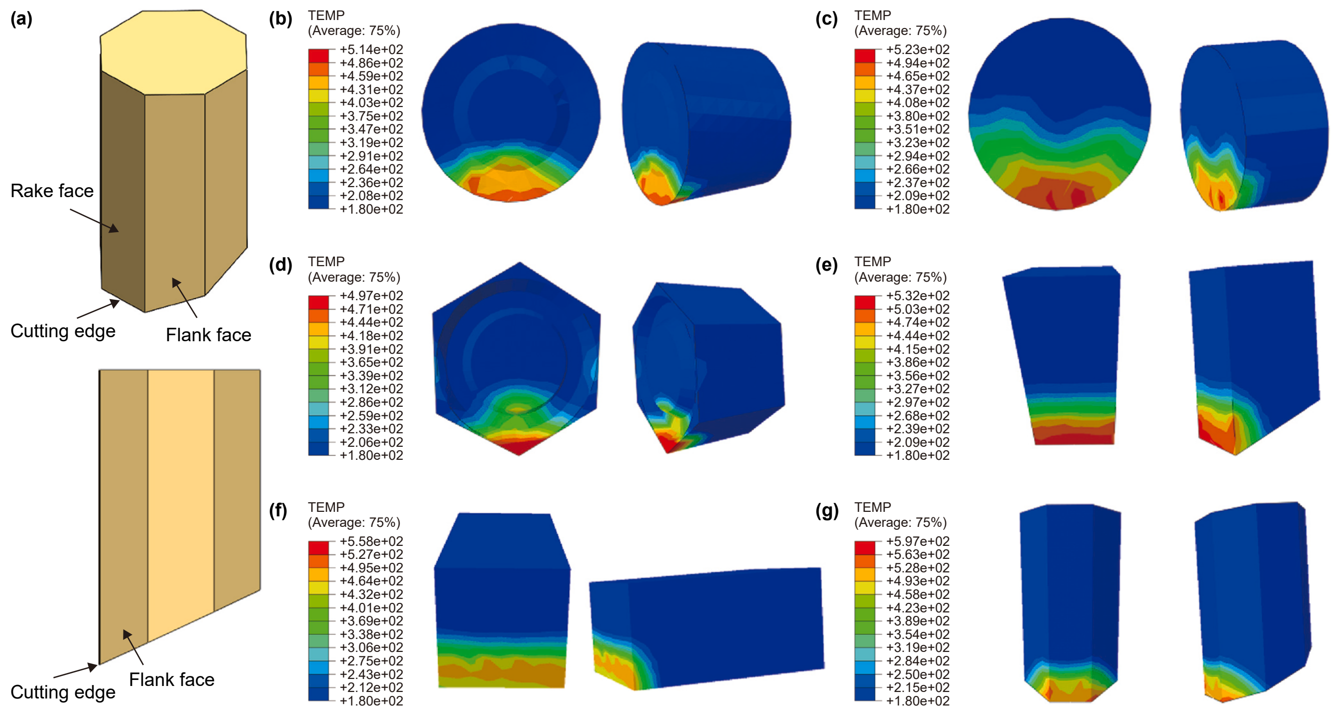

Fig. 12. Temperature distribution characteristics of various abrasive grains. **(a)** Abrasive grain structure diagram; **(b)** Disc abrasive grain; **(c)** Cylindrical abrasive grain; **(d)** Honeycomb abrasive grain; **(e)** Pointed teeth abrasive grain; **(f)** Long strips of abrasive grain; **(g)** Prismatic abrasive grain.

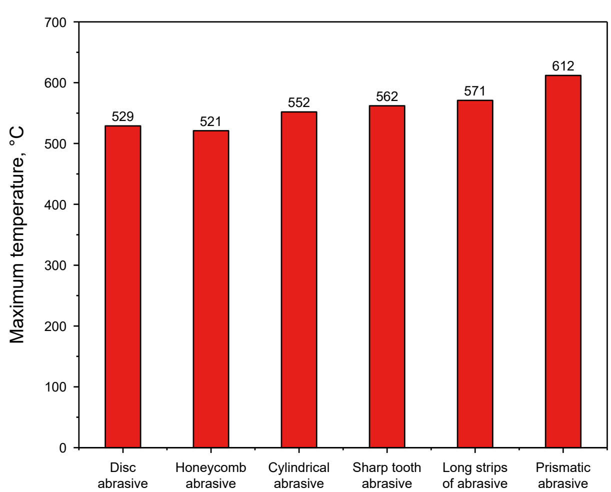

Fig. 13. Graph of the highest temperatures of various abrasive grains.

blockages in the well, and they are prone to generating local high temperatures, causing the abrasive grain to fail and thereby reducing the service life of the drilling bit for workover. Therefore, in the high-temperature environment of the deep wellbore, to ensure that the drilling bit for workover has a longer service life, honeycomb abrasive grain or disc abrasive grain should be used. Their textured structure can increase the heat dissipation area and effectively prevent the accumulation of local heat on the front cutting surface of the abrasive grain.

5.4. Analysis of work efficiency

The breakage work is an important indicator for evaluating the efficiency of abrasive grains from the perspective of energy. The breakage work refers to the energy consumed by abrasive grains when cutting a unit volume of material (Kishawy et al., 2004; Zhang et al., 2015). During the abrasive cutting process, energy conversion occurs in three deformation zones. The energy provided by the drill pressure and torque is transformed into the elastic-plastic deformation properties of the metal debris and chips in the first deformation zone, the friction heat between the chips and the rake face of the abrasive grain in the second deformation zone, the friction heat between the metal debris and the flank face of the tool in the third deformation zone, and the cohesive energy of the newly formed surface. The first deformation zone is the main deformation zone during the cutting process. The mechanical energy of the abrasive grain gradually converts into the deformation energy of the material, and the energy consumption is the highest (Ni and Zhu, 2014; Wang and Yang, 2022). The following will make a comparative evaluation of the abrasive grain work efficiency from the perspective of crushing work.

Based on the different structural type simulation models of abrasive grains established in the previous text, through the post-processing module of Abaqus, the quality attributes of the metal blockage after cutting were queried, and the volume of the metal blockage after cutting was extracted, as shown in Fig. 14. The difference between the volume of the metal blockage before cutting and that after cutting was calculated to obtain the volume of the removed material. At the same time, the ALLWK (external work) in the Abaqus post-processing module was output, which is the total energy consumed during the cutting process.

The breakage work of abrasive grain of different structural types is calculated using Eq. (9).

$$e = \frac{E}{V} \tag{9}$$

In the formula, e represents the crushing work of the material, E represents the total cutting energy, and V represents the total volume of material removed.

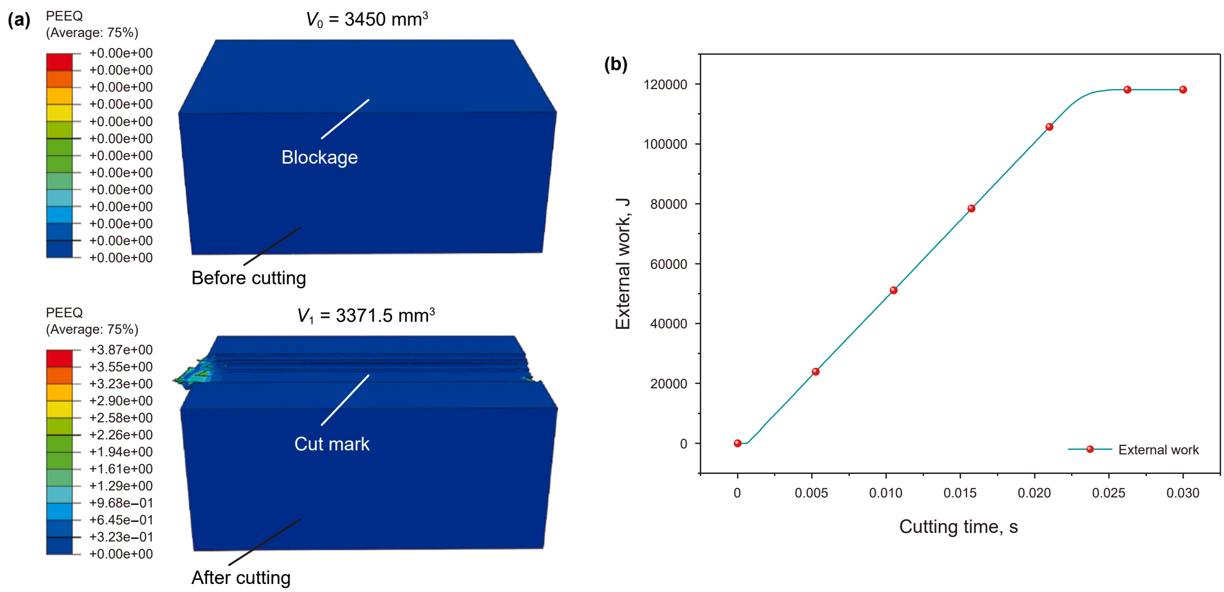

Fig. 14. Volume and energy consumption before and after cutting. **(a)** Volume change diagram; **(b)** External force doing work.

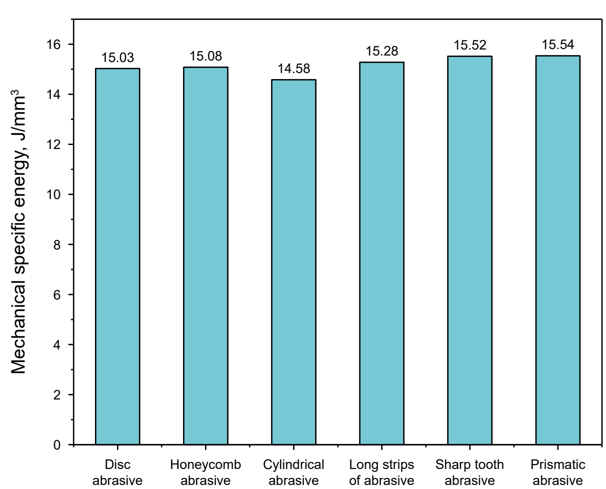

Fig. 15. Mechanical specific energy of various abrasive grains.

The breakage work diagrams of abrasive grain of different structural types were established, as shown in Fig. 15. From the power consumption diagrams of different structural types of abrasive grain, it can be concluded that under the same working conditions, when cylindrical abrasive grain cuts through metal obstructions, the energy consumed to cut a unit volume of material is the least, only 14.58 J per cubic millimeter. At the same time, the pointed teeth abrasive grain and the prismatic abrasive grain consume more energy during cutting, with 15.52 and 15.54 J per millimeter, respectively. Disc abrasive grain and honeycomb abrasive grain consume slightly more energy than cylindrical abrasive grain. Under the conditions studied, the cylindrical abrasive grains exhibited a tendency to form chips more easily during the cutting process, while the plastic work of material removal was relatively low. This made them show potential advantages in terms of cutting efficiency. Based on this, from the perspective of work efficiency, cylindrical abrasive grains can be regarded as a more efficient option.

6. Conclusions

This paper mainly focuses on the cutting characteristics of abrasive grains on metal blockages in the high-temperature environment of the deep wellbore. By integrating the research methods of theoretical analysis, finite element simulation and indoor experiments, it conducts a study on the cutting characteristics of different structural types of abrasive grains in the high-temperature environment of the deep wellbore, and reaches the following conclusions.

(1) The accuracy of the thermodynamic coupling simulation model of the abrasive grain on the drilling bit for workover is 9.98%, which can meet the basic engineering analysis accuracy requirements.
(2) From the perspective of work safety, the fluctuation range of cutting force during the cutting process of honeycomb abrasive grain and disc abrasive grain is relatively small, being 1.27 and 1.45 kN, respectively. When milling metal blockages in the high-temperature environment of the deep wellbore, it is conducive to ensuring the smooth operation of the drilling bit for workover and has higher safety and stability.
(3) From the perspective of work temperature, the temperature of the honeycomb abrasive grain is the highest, and that of the disc abrasive grain is the lowest, being 521 and 529 °C, respectively. When working in the high-temperature environment of the deep wellbore, the unique annular texture structure of the honeycomb abrasive grain and the disc abrasive grain can effectively dissipate heat, preventing the accumulation of heat and avoiding the formation of high temperatures that would alter the performance of the cutting tool material, thereby extending the service life of the drilling bit for workover.
(4) From the perspective of work efficiency, cylindrical abrasive grain causes the least fragmentation during cutting, with a fragmentation work of 14.58 J per cubic millimeter. Cylindrical abrasive grain is more likely to form chips during the cutting process. Under the same conditions, the plastic work

of the material is lower, resulting in higher cutting efficiency.

(5) Based on an analysis of work safety, work temperature and work efficiency, when cutting metal blockages in the high-temperature environment, the honeycomb abrasive grain is recommended as the preferred choice. The research content can provide theoretical guidance and technical support for the development of an efficient drilling bit for workover in the high-temperature environment of the deep wellbore.

(6) It is necessary to admit that the conclusions of this study were derived under idealized boundary conditions. We ignored the dynamic factor of downhole pipe column vibration and assumed that the microstructure of the metal material remained stable at 500 °C. Therefore, the differences in cutting performance of the different structural abrasive grains revealed by this study should be more accurately understood as the performance under the specific premise of “stable conditions and constant material properties”. Although this limitation enables us to focus more clearly on the influence of structural factors, it also means that when these conclusions are applied to actual deep well conditions with severe vibration or extreme temperatures causing material softening and phase transformation, their applicability may be constrained. Future research that can incorporate these dynamic and microscopic variables into consideration will be able to construct a more complete and closer-to-reality evaluation system for abrasive particle cutting performance.

CRediT authorship contribution statement

Jia-Qi Che: Conceptualization. **Jia-Qi Qiao:** Data curation. **Chang-Chang Chen:** Formal analysis. **Yi-Han Fan:** Investigation. **Yun-Fei Chen:** Methodology. **Yan-Wen Zhang:** Project administration. **Han-Xiang Wang:** Supervision.

Declaration of competing interest

The authors declare that they have no known competing financial interests or personal relationships that could have appeared to influence the work reported in this paper.

Acknowledgments

This work was supported by the Open Fund of Hubei Key Laboratory of Oil and Gas Drilling and Production Engineering (Yangtze University) under Grant No. YQZC202303, the National Natural Science Foundation of China under Grant No. 52304015, the Shandong Provincial Natural Science Foundation under Grant No. ZR2025MS838, and the Independent Innovation Research Project of China University of Petroleum (East China) under Grant No. 24CX06010A.

References

Abbas, R.K., 2018. A review on the wear of oil drill bits (conventional and the state of the art approaches for wear reduction and quantification). Eng. Fail. Anal. 90, 554–584. https://doi.org/10.1016/j.engfailanal.2018.03.026.

Che, J., Wang, H., Zhang, Y., et al., 2020a. Experimental study on the working performance of different milling tools for multistage fracturing ball seats. Pet. Sci. 17, 1699–1716. https://doi.org/10.1007/s12182-020-00492-4.

Che, J., Wang, H., Zhang, Y., et al., 2020b. Experimental and numerical studies on chip formation mechanism and working performance of the milling tool with single abrasive grain. J. Petrol. Sci. Eng. 195 (3), 107645. https://doi.org/10.1016/j.petrol.2020.107645.

Che, J., Wang, H., Zhang, Y., et al., 2020c. Field test and numerical simulation of the section mill in U-shaped wells of coalbed methane. J. Nat. Gas Sci. Eng. 84 (2-3), 103681. https://doi.org/10.1016/j.jngse.2020.103681.

Che, J., Zhang, Y., Wang, H., et al., 2021. A novel method for analyzing working performance of milling tools based on reverse engineering. J. Petrol. Sci. Eng. 197 (2), 107987. https://doi.org/10.1016/j.petrol.2020.107987.

Che, J., Zhang, Y., Wang, H., et al., 2023. An experimental and numerical study on the wear mechanism of cutters on workover bits under thermo-mechanical coupling. Geoenergy Sci. Eng. 224 (2), 211628. https://doi.org/10.1016/j.geoen.2023.211628.

Dai, X., Huang, Z., Shi, H., et al., 2022. Experimental investigation on the PDC cutter penetration efficiency in high-temperature granite. Geothermics 98, 102281. https://doi.org/10.1016/j.geothermics.2021.102281.

Kishawy, H.A., Kannan, S., Balazinski, M., 2004. An energy based analytical force model for orthogonal cutting of metal matrix composites. CIRP Ann. 53 (1), 91–94. https://doi.org/10.1016/S0007-8506(07)60652-0.

Larsen, A., Garfield, G., 2013. Advanced milling technology sets record for number of composite mill outs for ‘Plug-N-Perf’ completions in the Williston basin. In: SPE/IADC Middle East Drilling Technology Conference & Exhibition. https://doi.org/10.2118/166747-MS.

Ljustina, G., Larsson, R., Fagerström, M., 2014. A FE based machining simulation methodology accounting for cast iron microstructure. Finite Elem. Anal. Des. 80, 1–10. https://doi.org/10.1016/j.finel.2013.10.006.

Lei, Q., Weng, D., Luo, J., et al., 2019. Achievements and future work of oil and gas production engineering of CNPC. Petrol. Explor. Dev. 46 (1), 139–145 (in Chinese) https://doi.org/10.11698/PED.2019.01.14.

Lei, Q., Li, Y., Li, T., et al., 2020. Technical status and development direction of workover operation of PetroChina. Petrol. Explor. Dev. 47 (1), 155–162 (in Chinese) https://doi.org/10.11698/PED.2020.01.15.

Luo, M., Gao, D., Li, W., 2023. Thermal solid coupling numerical simulation of plastic mudstone fractured by special PDC cutting teeth. China Offshore Oil Gas 35 (2), 129–137 (in Chinese) https://doi.org/10.11935/j.issn.1673-1506.2023.02.014.

Lu, L., 2024. Petroleum economic news. Int. Pet. Econ. 32 (8), 106–108 (in Chinese) https://doi.org/10.3969/j.issn.1004-7298.2024.10.015.

Li, B., He, Z., Liang, C., et al., 2024. Dynamic rock-breaking temperature distribution of PDC bit cutter based on orthogonal cutting theory. China Min. Mag. 33 (4), 171–181 (in Chinese) https://doi.org/10.12075/j.issn.1004-4051.20230625.

Maczura, J.M., Miller, M., Scuadroni, N., et al., 2015. Effects of downhole parameters on horizontal milling applications. In: SPE Annual Technical Conference and Exhibition. https://doi.org/10.2118/174921-MS.

Ni, H., Zhu, G., 2014. Modeling of shear angle calculation based on minimum of plastic deformation energy. J. Anhui Univ. Technol. (Nat. Sci.) 31 (2), 120–125 (in Chinese) https://doi.org/10.3969/j.issn.1671-7872.2014.02.004.

Qian, M., Xiao, J., Wang, G., et al., 2020. Evaluation of heat generation using a microscopic cutting model with thermo-mechanical coupling for carbon fiber reinforced polymer composites. J. Reinforc. Plast. Compos. 39 (21-22), 793–804. https://doi.org/10.1177/0731684420931589.

Rajabov, V., Miska, S., Mortimer, L., et al., 2012. The effects of back rake and side rake angles on mechanical specific energy of single PDC cutters with selected rocks at varying depth of cuts and confining pressures. In: IADC/SPE Drilling Conference and Exhibition. SPE-151406-MS. https://doi.org/10.2118/151406-MS.

Rostamsowlat, I., Akbari, B., Evans, B., 2018. Analysis of rock cutting process with a blunt PDC cutter under different wear flat inclination angles. J. Petrol. Sci. Eng. 171, 771–783. https://doi.org/10.1016/j.petrol.2018.06.003.

Stowe, C., Ponder, A., 2014. High endurance cutting elements. In: IADC/SPE Drilling Conference and Exhibition. https://doi.org/10.2118/167944-MS.

Sun, L., Wu, S., Pan, G., et al., 2018. Analysis of three-dimensional mechanical model of single-tooth orthogonal cutting. Tool. Eng. 52 (11), 118–121 (in Chinese) https://doi.org/10.16567/j.cnki.1000-7008.2018.11.034.

Wang, Q., Qin, Y., Jia, W., et al., 2018. Density and viscosity of tight oil from Yanchang formation, Ordos basin, China and the geochemical controls. Petrol. Sci. Technol. 36 (16), 1298–1304. https://doi.org/10.1080/10916466.2018.1471495.

Wang, C., Li, S., Zhang, L., 2019. Evaluation of rock abrasiveness class based on the wear mechanisms of PDC cutters. J. Petrol. Sci. Eng. 174, 959–967. https://doi.org/10.1016/j.petrol.2018.12.009.

Wang, Y., Yang, S., 2022. Finite element analysis of the influence of heat source parameters on cutting performance. Mach. Des. Manuf. 3, 129–133 (in Chinese) https://doi.org/10.19356/j.cnki.1001-3997.20211115.010.

Xiao, S., Xiang, M., Guo, J., et al., 2024. Study on the Shearing Force of Ram and Fracture Characteristics of Drillpipe Under Precutting. SPE J. 29 (6), 2840–2856. https://doi.org/10.2118/219482-PA.

Yan, T., Li, W., Bi, X., et al., 2009. A new evaluation method for rock-crushing efficiency based on crushing work ratio. Acta Pet. Sin. 30 (2), 291–294 (in Chinese) https://doi.org/10.7623/syxb200902024.

Ye, W., Guo, Y., Liang, R., et al., 2019. Research on thermo-mechanical coupling deformation for the ball screw of machine tool spindle feed system. J. Vib. Eng. Technol. 8 (3), 443–454. https://doi.org/10.1007/s42417-019-00182-5.

Yang, M., 2022. A brief discussion on the characteristics of titanium alloy materials and their grinding features. Inf. Rec. Mater. 23 (1), 41–44 (in Chinese) https://doi.org/10.16009/j.cnki.cn13-1295/tq.2022.01.025.

Zhang, H., Kong, L., Li, T., et al., 2015. SCE modeling and influencing trend analysis of cutting parameters. China Mech. Eng. 8, 1098–1104 (in Chinese) https://doi.org/10.3969/j.issn.1004-132X.2015.08.019.

Zhu, X., Liu, W., 2018. Rock breaking and ROP rising mechanism of rotary-percussive drilling technology. Acta Pet. Sin. 39 (2), 216–222 (in Chinese) https://doi.org/10.7623/syxb201802010.

Zhang, J., Wang, G., He, K., et al., 2019. Practice and understanding of sidetracking horizontal drilling in old wells in Sulige gas field. Petrol. Explor. Dev. 46 (2), 370–377 (in Chinese) https://doi.org/10.11698/PED.2019.02.17.

Zhou, L., Wang, Z., Wen, H., 2019. On the accuracy of the Johnson-Cook constitutive model for metals. Chin. J. High Press. Phys. 33 (4), 042101 (in Chinese) https://doi.org/10.11858/gywlxb.20190721.

Zheng, M., He, C., Yang, S., 2020. Thermo-mechanical coupling behaviour when milling titanium alloy with micro-textured ball-end cutters. Proc. Inst. Mech. Eng. Part E Journal of Process Mechanical Engineering 234 (6), 095440892093195. https://doi.org/10.1177/0954408920931958.

Zhang, Z., Zhao, D., Zhao, Y., et al., 2020. Simulation and experimental study on temperature and stress field of full-sized PDC bits in rock breaking process. J. Petrol. Sci. Eng. 186 (1), 106679. https://doi.org/10.1016/j.petrol.2019.106679.